

# THE ALGORITHM OF EXTRACTING CYCLOGRAPHIC MAPS

*Ching-Shoei Chiang*

Computer and Information Science,  
Soochow University, Tappei, Taiwan, R.O.C.  
Email: [chiang@cis.scu.edu.tw](mailto:chiang@cis.scu.edu.tw)

## ABSTRACT

The cyclographic maps and its relation to offset curve, the medial axis transform is introduced in this paper. We also modify the cyclographic maps into the weighted cyclographic maps and extracting the weighted offset curves and weighted medial axis transform from it. Algorithm to extract the cyclographic map from the boundary curve is introduced.

### 1. Introduction – Offset Curve, Medial Axis Transform

There are 4 sections in this paper. The first section gives definitions for the curve and the oriented curve, introduces  $r$ -offset of the (oriented) curve, medial axis and medial axis transform associated with “one side” of a curve, or a closed domain. The second section describes the cyclographic maps. The third section describes the algorithm of extracting cyclographics and weighted cyclographics for an oriented curve, and the final section describes the relationship between cyclographics and offset curve, medial axis transform, and blending curves.

#### 1.1 Curves

**Definition 1** A curve in the real Euclidean space  $\mathbb{R}^2$  is a map  $\alpha: [a, b] \rightarrow \mathbb{R}^2$ , where  $\alpha(t) = (x(t), y(t))$  and  $x(t)$ ,  $y(t)$  are continuous functions. An oriented curve is a curve with orientation from  $\alpha(a)$  to  $\alpha(b)$ .

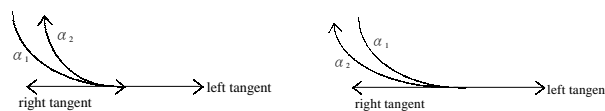
If  $\alpha$  is an oriented curve, we called the point  $\alpha(a)$  and  $\alpha(b)$  the start and end point of the oriented curve. If  $\alpha$  is a curve, we called both  $\alpha(a)$  and  $\alpha(b)$  end points.

**Definition 2** A (oriented) curve  $\alpha: [a, b] \rightarrow \mathbb{R}^2$  is:

- simple if  $\alpha$  is one-to-one.
- differentiable if  $d\alpha/dt$  is defined and not zero, for all  $t \in [a, b]$ , where  $d\alpha/dt$  is the derivative of  $\alpha$  by  $t$ .
- twice differentiable if  $d^2\alpha/dt^2$  is defined and not zero, for all  $t \in [a, b]$ , where  $d^2\alpha/dt^2$  is the second derivative of  $\alpha$  at  $t$ .
- closed if  $\alpha(a) = \alpha(b)$ .
- of bounded curvature variation if there are finitely many local extrema of the curvature. And, there are finitely many inflection points.

We define the right tangent and the left tangent of  $\alpha(t)$  as the vector from  $\alpha(t+\Delta t)$  to  $\alpha(t)$  and from  $\alpha(t-\Delta t)$  to  $\alpha(t)$

respectively, when the  $\Delta t$  approaches to zero. Let  $p$  be a point on the oriented simple curve  $\alpha$ , let  $\theta$  be the angle measured counter-clockwise from  $p$ 's left tangent to its right tangent. If  $\theta=0$ , the point  $p$  is a differentiable point. If  $0 < \theta < \pi$  or  $\pi < \theta < 2\pi$ , the point is a convex or concave vertex respectively. There are two cases for  $\theta=\pi$ . Consider the curve in Figure 1a and 1b, the point  $p$  separate the curve into two subcurves  $\alpha_1$  and  $\alpha_2$ ,  $\alpha_1$  is from start point to  $p$  and  $\alpha_2$  is from  $p$  to the end point. If  $\alpha_2$  is locally in the “left-side” of  $\alpha_1$  at  $p$  (Figure 1a), then  $p$  is a convex vertex. If  $\alpha_2$  is locally in the “right-side” of  $\alpha_1$  at  $p$  (Figure 1b), then  $p$  is a concave vertex. If  $\alpha_1$  is locally equal to the  $\alpha_2$ , the curve  $\alpha$  will not be simple. We only consider simple curve with bounded curvature variation in this paper.



(a) Convex

(b) Concave

Figure 1 Convex/concave with opposite tangent direction

The right normal vector and left normal vector are further defined as the right tangent and left tangent vectors which rotated 90 degree counter-clockwise. The negative left normal of  $\alpha$  at  $p$  is the left normal with reverse direction. The negative right normal and the negative normal are defined similarly. There is no left and right normal for the start and end points of  $\alpha$  respectively.

Notice that for the differentiable point  $p$ , its left tangent is equal to its right tangent, and its left normal is equal to its right normal. We simply call them the tangent of  $p$  or the normal of  $p$ . We treat the start and end point are differentiable points. Their tangents (normals) are right tangent (normal) and left tangent (normal) respectively.

The left(right) side of the oriented simple curve  $\alpha$  at  $p$  is defined as follows:

- If the point  $p$  is differentiable, the left(right) side of  $\alpha$  at  $p$  is the normal(negative normal) of  $\alpha$  at  $p$ .
- If the point  $p$  is a convex point, the left(right) side of  $\alpha$  at  $p$  is the area span by the vectors rotated counter-clockwise from the (negative) left normal at  $p$  to the (negative) right normal at  $p$ .

- If the point  $p$  is a concave point, the left side of  $\alpha$  at  $p$  is the area span by the vectors rotated clockwise from the (negative) left normal at  $p$  to the (negative) right normal at  $p$ .
- The left(right) side of an oriented simple curve  $\alpha$  is the union of the left(right) side of  $\alpha$  at all points on  $\alpha$ .

Notice that under these definitions, the left(right) side of an open oriented curve is not necessary bounded.

## 1.2 Offset Curves

We introduce the notions of local distance, global distance, local offset and global offset in this section.

Given a plane curve  $C$ , its offset by a distance  $r$  is a curve  $Off(C,r)$  such that the points of  $Off(C,r)$  are at distance  $r$  from  $C$ . These informal definitions can be made more precise in one of two ways, depending on whether the distance is measured locally or globally. Denote the Euclidean distance of two points  $p$  and  $q$  with  $d(p,q)$ . Let  $C$  be a curve in  $R^2$ , and  $p$  any point. Define the global distance of  $p$  to  $C$  by

$$dist_g(p,C) = \{d(p,q) \mid q \in C \text{ and } d(p,q) \text{ has global minimal}\}$$

where  $d(p,q)$  is the Euclidean distance of two points. For a smooth curve  $C$ , a local distance can be defined as

$$dist_l(p,C) = \{d(p,q) \mid q \in C \text{ and } d(p,q) \text{ has extreme value}\}$$

Notice that  $dist_g(p,C) = \min \{dist_l(p,C)\}$

From [1], we know that if  $q$  is not end point of the curve  $C$ , and  $C$  is differential at  $q$ , then  $pq$  is perpendicular to the tangent of  $C$  at  $q$ . For most reasonable curves  $C$  these definitions make sense. Notice that  $dist_g(p,C)$  is a singleton and  $dist_l(p,C)$  may have more than one element.

Given a parametric or implicit representation of the curve. the local and global offsets can be defined as follows [2, 3,4]. In the global offset, the global distance is used, so that

$$Off_g(C,r) = \{p \in R^2 \mid r \in dist_g(p,C)\}$$

Local offsets are simple to define analytically, That is,

$$Off_l(C,r) = \{p \in R^2 \mid r \in dist_l(p,C)\}$$

Moreover, the local offset of an algebraic curve or surface again is an algebraic curve. Notice that the offset of a curve has two components for a curve, each one on the different side of the curve. We restricted the offset of an oriented curve to be the offset on its left side.

## 1.3 Offsets for an oriented simple curve

Let us consider the offset for the oriented curve  $\alpha$ . We give distance with sign on the oriented curve. For the point at the left(right) side of  $\alpha$  at  $p$ , its distance to  $p$  is positive(negative). Notice that there exist points on both sides of  $\alpha$ , as the point  $q$  in Figure 2. We call that  $p_1$  is  $q$ 's footpoint on  $\alpha$  from  $q$ 's right side, and  $p_2$  is  $q$ 's footpoint on  $\alpha$  from  $q$ 's left side. Or,  $q$  is on left side of  $\alpha$  at  $p_1$ , and  $q$  is on right side of  $\alpha$  at  $p_2$ .

The local and global distance for point to oriented curve are defined as:

$$dist_l^+(q,\alpha) = \{d(p,q) \mid p \in \alpha; d(p,q) \text{ has extreme value}; \text{ and } q \text{ is on the left side of } \alpha \text{ at } p\}$$

$$dist_l^-(q,\alpha) = \{-d(p,q) \mid p \in \alpha; d(p,q) \text{ has extreme value}; \text{ and } q \text{ is on the right side of } \alpha \text{ at } p\}$$

$$dist_g^+(q,\alpha) = \min \{dist_l^+(q,\alpha)\}$$

$$dist_g^-(q,\alpha) = \max \{dist_l^-(q,\alpha)\}$$

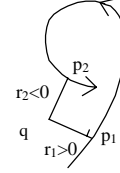


Figure 2 points on both sides of  $\alpha$

Let's consider the  $r$ -offset for an oriented simple curve now. If  $r > 0$  ( $r < 0$ ), the  $r$ -offset of  $\alpha$  is the trace of points that is in the left(right) side of the curve, and its distance to the curve is equal to  $r$ . This  $r$ -offset can be global or local, depend on the local global distance or local distance we use. Under this definition, if  $\beta$  is the same as  $\alpha$  except that  $\beta$  is not oriented, the union for the  $r$ -offset and  $-r$ -offset of  $\alpha$  is not equal to the  $r$ -offset of  $\beta$ . The only difference is at the start and end point of the curve  $\alpha$ . The offset of contains circular arc at the start and end point, the  $r$ -offset of  $\alpha$  is the intersection of  $r$ -offset of  $\beta$  and the left side of  $\alpha$ . Similarly, the  $-r$ -offset of  $\alpha$  is the intersection of  $r$ -offset of  $\beta$  and the right side of  $\alpha$ .

The local and global offsets of an oriented curve are defined as:

$$Off_g(\alpha,r) = \{p \in R^2 \mid r \in dist_g^+(p,\alpha) \text{ or } r \in dist_g^-(p,\alpha)\}$$

$$Off_l(\alpha,r) = \{p \in R^2 \mid r \in dist_l^+(p,\alpha) \text{ or } r \in dist_l^-(p,\alpha)\}$$

In the above definition, if the point  $p$  is not on the left side and right side of  $\alpha$ , we defined  $dist_l^+(p,\alpha)$  and  $dist_l^-(p,\alpha)$  are equal to  $\infty$  and  $-\infty$  respectively.

It is possible that a point is both on the positive and negative offset of  $\alpha$ , as the point  $p$  in Figure 2. The point  $q$  is on both  $+r$ -offset and  $-r$ -offset of  $\alpha$  when  $r = r_1 = -r_2$ .

If  $C$  is the curve  $\alpha$  without orientation, we have

$$Off_g(\alpha,r) \in Off_g(C,|r|)$$

$$Off_l(\alpha,r) \in Off_l(C,|r|)$$

The proof is base on the fact that there are more restriction to define  $dist_g$  and  $dist_l$  for oriented curve than curve.

Consider the curve  $C$  with the implicit equation  $f(x,y)=0$ . Let  $(u_1,v_1)$  be a point on  $f$  and  $(x,y)$  be a point on the normal of  $f$  at  $(u_1,v_1)$ . Let  $f_x$  denote the differential of  $f$  with respect to  $x$ . In 2D, the system of equation for the local offsets with distance  $d$  to the boundary in the dimensionality paradigm is [6]:

$$f(u,v) = 0$$

$$f_x(y-v) - f_y(x-u) = 0$$

$$(x-u)^2 + (y-v)^2 = d^2$$

The first equation states that the point  $(u_i, v_i)$  is on  $f$ . The second equation assures the fact that  $(x, y)$  is on the normal of  $f$  at  $(u_i, v_i)$ . And, the third equation asserts that the distance from the boundary curve to offset curve is equal to  $d$ . Notice that in the general case, the degree of freedom is 1, so that the offset of the curve should be a curve in 2D.

With similar approach, we can generate the system of equation for the curve with parametric form. Consider the curve  $C(t)=(X(t), Y(t))$ , we have the following system of equation:

$$\begin{aligned} (x-X(t))*X_t(t)+(y-Y(t))*Y_t(t) &= 0 \\ (x-X(t))^2+(y-Y(t))^2 &= d^2 \end{aligned}$$

We can eliminate the variable to find the implicit form for the offset curve [22].

The properties of the 2D offset curves is well introduced in [24,25]. There are also many algorithms to extract 2D offsets, such as [26,27].

#### 1.4 Medial Axis and Medial Axis Transform

Consider a compact region in  $R^2$ . There are two equivalent definitions for the medial axis (MA) of such region, namely:

**Definition 3** (Blum) The internal medial axis (or skeleton) of a 2D compact region is the closure of the locus of the centers of all maximal disks which are contained in the shape.

**Definition 4** Let a footpoint of  $p$  be a point  $p'$  on the boundary of a 2D region that has minimum distance to  $p$ . The interior medial axis of a 2D closed region is the closure of the locus of the points inside the region which have more than one footpoint.

Let's extend the definition 4 into noncompact 2D region. Consider an oriented curve with its left side as the 2D region, the medial axis of this 2D region is the closure of the locus of the points inside the region which have more than one footpoint. Notice that under this definition, the line connecting the point  $p$  with its footpoint  $p'$  will be perpendicular to the tangent of the boundary curve at  $p'$ .

We can define the  $MAT^+$  and  $MAT^-$  for oriented curve. The  $MAT^+$  of the oriented curve  $\alpha$  is the closure of the set of points which are located on the right (left) of  $\alpha$  and have two or more footpoints on  $\alpha$  from their left (right). Consider the point  $q$  on Figure 2. Although  $q$  is on the left side of  $\alpha$  (and also the right side of  $\alpha$ ), there are only one footpoint  $p_1$  on  $\alpha$  from its right, so the point  $q$  is not belong to  $MAT^+$  of  $\alpha$ . More formally, we have:

$$MAT^+(\alpha) = \text{closure}\{q \mid q \text{ is on the left side of } \alpha; q \text{ has more than one footpoints on } \alpha \text{ from } q's \text{ right side} \}$$

$$MAT^-(\alpha) = \text{closure}\{q \mid q \text{ is on the right side of } \alpha; q \text{ has more than one footpoints on } \alpha \text{ from } q's \text{ left side of } \alpha \}$$

The function which maps an MA point to the distance between the MA point and its footpoints is called the radius function. The medial axis and the associated radius function define the medial axis transform (MAT). The definition

extends naturally to the concept of a left(right) MAT associated to the left(right) side of an oriented curve.

There are many applications of the MAT of 2D regions. The interior MAT can be used in shape representation and shape recognition [7,8,9,10,11,12], especially for objects whose width is relatively unimportant such as characters in character recognition, or chromosomes in microbiology. The medial axis has also been used in finite-element mesh generation [13,14,15,16]. Many global shape characteristics can be extracted from the internal MAT of the shape, as explained in [13]. The external MAT can be used in motion planning [17]. For example, the external MAT of  $n$  obstacles can be used to define a collision-free path for robots that maximizes clearance from the obstacles. The MAT is also useful in casting design [18] and has potential applications in geometric tolerancing [19].

The properties of 2D MAT can be found in [28, 30]. There are also many algorithms to extract 2D MAT, such as [28, 29].

#### 2. Cyclographics and Weighted Cyclographics

Cyclographic maps have been introduced in [20] and used in computer science [19]. Every point in  $(x, y, z)$ -space is associated with an oriented circle in the  $(x, y)$ -plane by making the point the vertex of a double right cone whose axis is parallel to the  $z$ -axis and intersecting the cone with the  $(x, y)$ -plane. If the point has a  $z$ -coordinate greater than 0, the orientation of the circle is counterclockwise, otherwise, the orientation of the circle is clockwise. Consider an oriented curve  $C$  in 2D, and rotate all of its normals 45 degrees about the tangent. Then we obtained a ruled surface called the cyclographic map  $S(C)$  of  $C$ . The projection of the self-intersection points of the surface onto the  $(x, y)$ -plane contains the MA of the curve. The internal MA is produced on one side (the side with  $z$  value greater than 0) and the external MA on the other side ( $z < 0$ ). If we do not care about the orientation of the circles, we can think of the cyclographic maps in another way. Let  $D$  be a closed simple domain, and consider the single cones whose apex is on the boundary and whose axis is parallel to the  $z$ -axis where the interior of the cone is in the  $z > 0$  region. Then, the envelope of the cones in the region  $z \geq 0$  is a different new cyclographic map. The only difference is that the new map is in the positive  $z$ -half space. The MAT is obtained in the set of the self-intersection points of the envelope. The internal MAT and the external MAT are all on the same side of the  $(x, y)$ -plane. Consider all cones whose apex is on the MAT and whose axis is parallel to the  $z$ -axis. The union of all the circles that are the intersection of the cones with the  $(x, y)$ -plane are then the original domain  $D$ . The plane  $z=r$  intersections with the maps produce the local  $r$ -offset of the original domain. Notice that every point in the half space  $z \geq 0$  corresponds to a right cone in 3D or a circle on  $(x, y)$ -plane, which means that three dimensional half-space can be represented by the set of circles in the plane. This notion that space could be treated as a collection of elements other than points was proposed by Plucker over 100 years ago [21].

We can restrict the surface  $S(C)$  such that it is the graph of a

function with the  $(x,y)$ -plane its domain. With each point  $(x,y)$ , we associate the minimum  $|r|$ , so that the point  $(x,y,r)$  is on  $S(C)$ . Let us call this surface the trimmed cyclographic map of  $C$ . The surface so defined is then the distance surface of Blum [7]. It follows, that the trimmed cyclographic map of  $C$  can be determined approximately with the Euclidean distance transform.

Notice the trimmed cyclographic map of  $C$  can be obtained from the cyclographic map of  $C$ . The cyclographic map can be easily extended to any closed domain with an oriented curve as its boundary, such as domains with holes. Figure 3(b)(c) shown examples of the cyclographic map and the trimmed (modified) cyclographic of the boundary curve of Figure 3(a).

Notice that the rotated normal of a differentiable point  $q \in C$  is a line for the cyclographic map of  $C$  and could be a line, half-line, or line segment for the trimmed cyclographic map of  $C$ .

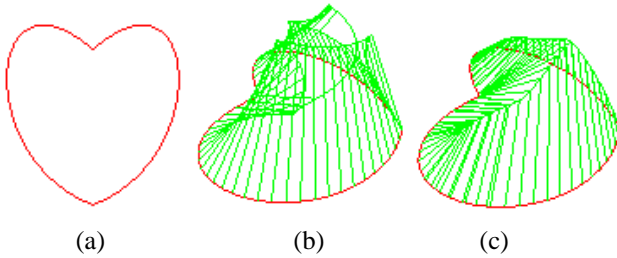


Figure 3 (a) The Curve (b) Cyclographic (c) Trimmed Cyclographic

In the cyclographic map, every rotated normal has 45 degree with  $z=0$  plane. The weighted cyclographic map is defined similar to cyclographic except that the degree between the rotated normal and  $z=0$  are varied. We define the degree function  $w(t)$  be the degree of the rotated normal along the oriented curve with  $z=0$  plane. We use the similar way to define the trimmed weighted Cyclographic maps. The weighted local (global)  $r$ -offset curve is defined as the intersection of  $z=r$  plane with weighted (trimmed weighted) cyclographic maps. The weighted MAT of the left region of an oriented curve is obtained in the self-intersection of its rotated normals.

## 2. Algorithm for extracting Cyclographic maps of oriented curve

We describe the algorithm which extracting cyclographic maps of oriented curve in this section.

Given a closed bounded domain, we would like to produce its trimmed cyclographic maps, so that the global weighted offsets of the boundary curve, weighted MAT of this closed domains, etc., can be easy extract from the cyclographic maps. The boundary curve is represented by a list of the boundary point with its associated rotated normals. We generated the cyclographic maps via two algorithms. The first one produce the cyclographic map and the second one produce the trimmed cyclographic map.

### Algorithm 1: Cyclographic map

1. Input the boundary curve using the piecewise cubic Bezier curve  $C_i(t)$ ,  $1 \leq i \leq m$ .

2. Find  $n$  intermediate points  $p_{i,j}$ ,  $1 \leq j \leq n+2$ , for each curve  $C_i(t)$  and each concave and concex vertex. Further, find the rotated normal for all of the point  $p_{i,j}$ . Reorder the boundary point into a list  $Q=[q_i]$ .

The above algorithm produce the rotated normal of all boundary points, we can display the cyclographic maps easily from the boundary curve points associated with its rotated normal, as shown in Figure 3b.

In order to find the trimmed cyclographic map, we have to find its self-intersection curve, and trim the cyclographic map. We use the divided and conquer strategy as the following:

### Algorithm 2: Trimmed Cyclographic Maps

1. Input the boundary curve using the piecewise cubic Bezier curve  $C_i(t)$ ,  $1 \leq i \leq m$ .

2. Find  $n$  intermediate points  $p_{i,j}$  for each curve  $C_i(t)$  and each concave and concave vertex. Furthermore, find the rotated normal for all of the point  $p_{i,j}$ . Reorder all of the boundary points into a list  $Q=[q_i]$ .

3. Let  $q_2$  as the starting boundary point, find its associated MAT point  $q$  and  $q$ 's other footpoints. If the other footpoints is not one of  $q_j$ ,  $j \neq i$ , and between  $q_i$  and  $q_{i+1}$ , then we insert one more boundary point  $q_k$  between  $q_i$  and  $q_{i+1}$  with its rotated normal in the list of points  $Q$ .

4. Separate the list  $Q$  into two (or more, if the first MAT points we find is a branch point) lists via the MAT point  $q$  and its footpoints  $q_2$  and  $q_k$ .

5. Push all of the lists into a queue.

6. If the queue is empty, go to 9. Otherwise, pop a list from queue. March along the MAT curve via the lists of points and associated MAT curve. Mark the boundary points after visit the boundary point.

7. If the MAT curve hit a branch point, subdivide the domain (point list) into three or more subdomains (point lists). Go to 5.

8. If the MAT curve hit an end point, go to 6.

9. Stop.

After the above algorithm, every rotated normal is bounded by an MAT point. The trimmed cyclographic maps is also easy to display, as shown in Figure 3c. Notice that the trimmed cyclographic maps produce extra boundary points in the third step in Algorithm 2, as we can see in the figure. Notice also that if we modify the algorithm, so that the rotated normal is a line instead of vector, and trim the rotated normal on both side, we can produce not only the internal MAT but also external MAT.

We answer the following questions steps by steps:

1. How to find the associated MAT and other footpoints (Step 3)?

Let  $q_2$  as the starting boundary point, We would like to find

its associated MAT point  $q$  and other footpoints. Consider the rotated normal of  $q_2$  and other rotated normals. Two consequence points with its rotated normal produce a bilinear surface. Because this two points are closed to each other, we can use a plane  $P$  to approximate the bilinear surface. If the rotated normal of  $q_2$  intersect the plane  $P$ , then there is a MAT point on the plane  $P$ , we would like to find the intersection of the rotated normal of  $q_2$  and the plane  $P$ . Sometimes there are more one such plane, we would like to find the plane whose intersection point is near than others. That is, its  $z$ -value is smaller.

The intersection points are found by:

1. Do coordinated transformation so that  $q_2$  is the original, Tangent of  $q_2(T(q_2))$  is along the  $X$ -axis, and the rotated normal of  $q_2(RN(q_2))$  is along the  $Y$ -axis. Now the original curve on  $XY$  plane becomes on the  $Y=-Z$  plane.
2. Find the intersection points of other ordered rotated normals with the new  $XY$  plane, call them  $r_i$ . If the sign of the  $x$ -coordinates of the intersection points varies from the point  $q_i$  to  $q_{i+1}$ , then the MAT points must bounded by the plane with  $RN(q_i)$ ,  $RN(q_{i+1})$  as its two boundaries. The points  $r_i$ , and  $r_{i+1}$  are two intersection points of  $RN(q_i)$ ,  $RN(q_{i+1})$  with the new  $XY$ -plane.
3. Find the  $z$ -value of the MAT points by calculating the intersection point of the line segment  $r_i r_{i+1}$  and the  $Y$ -axis. After that, we can find a intermediate point between  $q_i$  and  $q_{i+1}$ , call it  $q'_i$ , by linear interpolation.

Let's introduce the idea more details, consider the point  $q_2$  as one of the points in an ellipse, as shown in Figure 4. The point  $q_2$  has local maximal curvature (Figure 4a), local minimal curvature (Figure 4c) or monotone increasing curvature from one side and monotone decreasing curvature from the other side (Figure 4c). After coordinated transformation,  $q_2$ ,  $T(q_2)$  and  $RN(q_2)$  become the origin, the  $X$ -axis and the  $Y$ -axis. The rotated normal vectors of other point of the ellipse intersects the new  $XY$ -plane are display in Figure 4d, Figure 4e, and Figure 4f, respectively. Notice that in Figure 4a and Figure 4d, we find an end MAT point because we cannot find any other rotated normal vectors intersect the  $XY$ -plane with smaller  $z$ -value. In Figure 4b, Figure 4c, Figure 4e and Figure 4f, a normal MAT point is found.

## 2. How to march along the MAT curves (Step 6)?

After we subdivide the domain, we have subdomains represented by lists of boundary points with its rotated normal vectors. Assume the half domain are represented by points  $[p_i]$ , and the first MAT point  $q$  and it footpoints are  $p_1$  and  $p_n$ , we would like to march along the MAT curves. Consider the neighbor points of  $p_1$  and  $p_n$ , there are three case it may happen (Figure 5)

- $RN(p_2)$  passing through the plane bounded by  $RN(p_n)$  and  $RN(p_{n-1})$  (Figure 5a).
- $RN(p_{n-1})$  passing through the plane bounded by  $RN(p_1)$  and  $RN(p_2)$  (Figure 5b).
- $RN(p_2)$  intersects  $RN(p_{n-1})$  (Figure 5c).

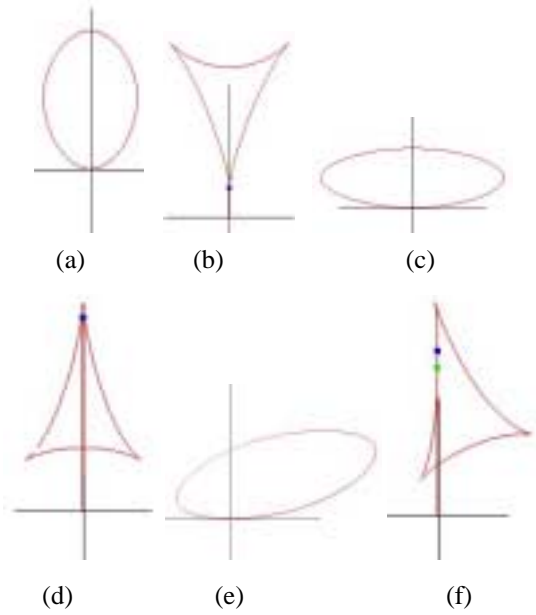


Figure 4 Finding the MAT point associated with a boundary point of an ellipse (a) maximal curvature point (b) intersection points (c) minimal curvature point (d) intersection points (e) normal point (f) intersection points

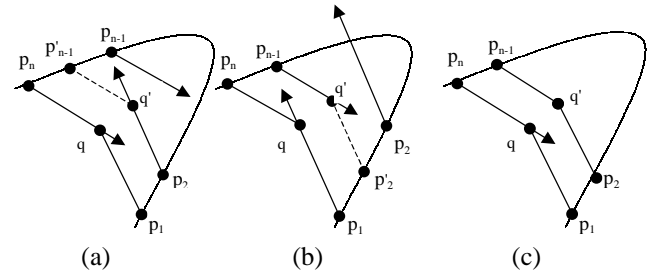


Figure 5 Marching along the MAT curve

We can find a new MAT point  $q'$ , new boundary points  $p'_{n-1}$  between  $p_{n-1}$  and  $p_n$  in the first case. After that, we mark the boundary points  $p_2$  and  $p'_{n-1}$ , and continue the steps of marching from the new MAT point  $q'$  and its footpoints  $p_2$  and  $p_{n-1}$ . We can process similarly for the second case. In the third case, we can find the intersection points  $q'$  as the MAT points, mark the boundary point  $p_2$  and  $p_{n-1}$ , and continue the marching start from the MAT points  $q'$  with its footpoints  $p_2$  and  $p_{n-1}$ .

## 3. How to judge the MAT curve hit the branch points (Step 7)?

After a few step of marching, we can do the step 1 again, and find all of the other points intersected by the remainder ordered rotated normal, generate the line segment connected the points. If there is a line segment intersect the  $Y$ -axis at  $q'$ , and the  $z$ -value of  $q'$  is less than the  $z$ -value of current MAT point, than we know we have been go too far for the MAT curve. In this case, we have to go back a few steps, unmark the boundary points and MAT points, find the MAT branch point, and subdivide the subdomain.

## 4. How to find the MAT branch points?

In the previous question, we find the MAT curve goes too far, we will do backtracking. For each backtracking, we do the coordinate transformation and find all the intersection point by the rotated normal vectors of the point in the list and the XY-plane. In the process, we may find the Y-axis intersect two or more bilinear surface generated by consequence rotated normal of boundary points. If the minimum two points whose z-value is near (say its distance less than or equal to a epsilon value)(shown in Figure 6(a)(b)), the branch points can be bounded by the intersection of three bilinear surface, one bilinear is bounded by  $RN(p_i), RN(p_{i+1})$ , another bilinear surface is bounded by  $RN(p_j), RN(p_{j+1})$ . The third bilinear surface may be bounded by  $RN(p_i), RN(p_2)$  or  $RN(p_2), RN(p_3)$ , assume the current boundary point we are working with is  $p_2$ .

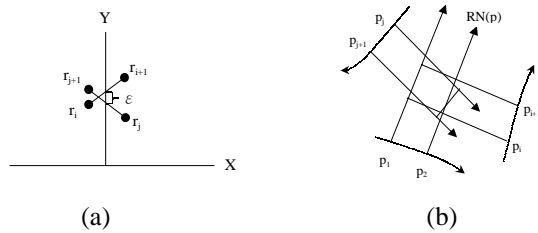


Figure 6 Extract the branch from the intersection of three bilinear surface

#### 5. How to terminate at the end point (step 8)?

We may check whether the list of points are marked or not. If all of the boundary points in the subdomain are marked, then we are probably near the end point. We may check the distances between the unmark point and its two neighbors, if the distance is less than  $\epsilon$ , then we quit the process by connect the unmark points with the final MAT point. Otherwise, we insert more boundary between the unmark point and its two neighbors, and continue to march along the MAT curve.

We have implemented the algorithms in PC using Visual C++ and OpenGL on Windows 98 and Windows NT. There are about 1,000 lines for the coding of GUI and another 1,000 lines for the ideas of the algorithms.

### 4. Application of the Cyclographic Maps

We introduce the applications of the Cyclographic Maps in this section. We introduce its relationship with offset curve and with MAT in the first subsection. In the second subsection, we modify the algorithm a little bit on the convex and concave vertices, so that the algorithm extend to handle the curve with singular points. The example for the boundary curve which is closed curve with hole is shown in the third subsection. The fourth subsection introduce the idea that convert the MAT curve back to the origin boundary curve. The final subsection introduce the way we can use cyclographic maps to do corner blending on singular points of curves.

#### 4.1 The relationship between cyclographics and offsets, MAT, and blending curve.

We summarize the relationship between cyclographic maps

with offset curves, medial axis transform and blending in this section by the examples shown below.

Using a Bezier curve generated by the control points  $(-2.0, 1.0, 0.0), (-1.5, -2.5, 0.0), (1.5, -2.5, 0.0)$  and  $(2.0, 3.0, 0.0)$  as the oriented curve  $\alpha$  we consider (shown in Figure 7a), we produce its cyclographic map (Figure 7b), trimmed cyclographic map (Figure 7c), and left local offsets  $Off_l(\alpha, r)$  (Figure 7d); left global offsets  $Off_g(\alpha, r)$  (Figure 7e); left medial axis transform  $MAT^+(\alpha)$  (Figure 7f).

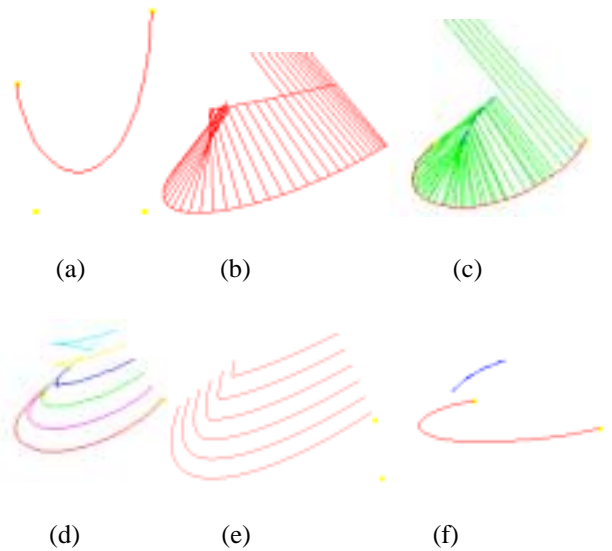


Figure 7 (a) The oriented curve (b) The cyclographic map (c) The trimmed cyclographic map (d) left local r-offset curves (e) left global r-offset curves (f) left MAT

In the mean time, we give the weight function as  $\omega(t) = (1-t) * 30^\circ + t * 60^\circ$ , where  $\omega(t)$  is the angle between the rotated normal and the  $z=0$  plane, and produce the weighted cyclographic map (Figure 8a) and trimmed weighted cyclographic map (Figure 8b), local weighted r-offset curve (Figure 8c), global weighted r-offset curve (Figure 8d) and weighted medial axis transform (Figure 8e).

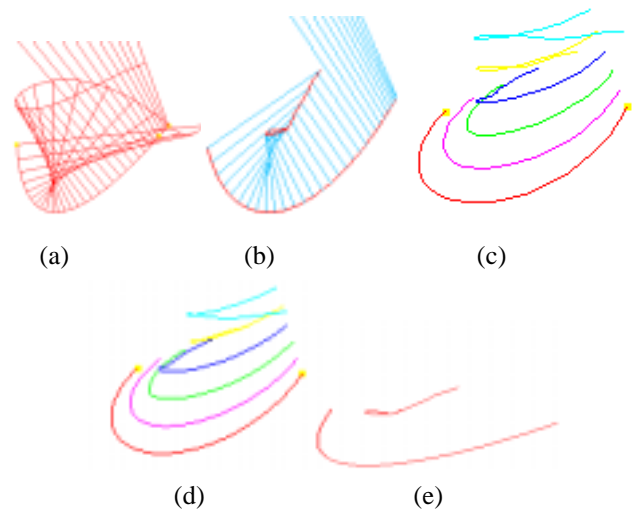


Figure 8 (a) The weighted cyclographic maps (b) the trimmed weighted cyclographic maps (c) left weighted local r-offset curves (d) left weighted global r-offset curves (e) left weighted medial axis transform

#### 4.2 Cyclographic Maps at the concave/convex vertex

The cyclographic maps at the concave/convex vertex can be trivially produced. We can produce partial cone whose apex is on the convex/concave vertex from the left rotated normal to the right rotated normal. It is a little complex for the weighted cyclographic maps. We have to blend the normal from left rotated normal to the right rotated normal, which means we have to produce a smooth “cone-like” surface to connect two surface produce by two curve to and from the vertex. There are various ways to do the blending, and we select the simply one. That is, we try to do the linear interpolation with the weighted function between the left rotated normal and the right rotated normal. The cyclographic map for convex vertex can be observed from Figure 8 to Figure 9, start from the plane  $z=r$  to  $z=r'$ , where  $r'>r$  and  $r$  is the radius of the osculating circle in the point which has local maximal curvature [23]. The cyclographic map for the concave vertex is shown in Figure 9 (a) to (e). This concave vertex is the intersection point of two curve generated by two Bezier Curve with control points at  $(-3.5, -3.0, 0.0), (-3.0, -2.0, 0.0), (-2.0, 0.0, 0.0), (-1.0, 0.5, 0.0)$  and  $(-1.0, 0.5, 0.0), (0.0, 0.0, 0.0), (1.0, -2.0, 0.0), (1.5, -3.0, 0.0)$  respectively. For the weighted cyclographic map, the weighted function for the first and second curves are  $\omega(t)=(1-t)*30^\circ+t*40^\circ$  and  $\omega(t)=(1-t)*50^\circ+t*70^\circ$  respectively. The (weighted) cyclographic map, (weighted) local offset curve and (weighted) global offset curve, (weighted) medial axis transform are displayed.

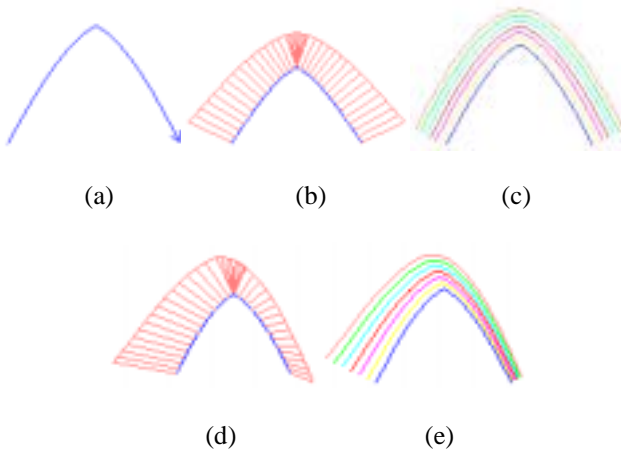


Figure 9 (a) The concave vertex of an oriented curve (b) Concave vertex in Cyclographic map (c) local (global) offset (d) concave vertex in Weighted cyclographic maps (e) weighted local (global) offset in the concave vertex.

#### 4.3 Cyclographic Maps for closed simple curve

Consider the cyclographic maps for the closed simple curve. The left side of the closed simple curve is bounded, so the medial axis transform is connected with or without loops[28]. But the weighted medial axis transform for closed region is not necessary connected without loop. We may use the same algorithm we mentioned before for weighted medial axis transform, the only difference is the part we calculated at the rotated normal of the boundary

points. The output cyclographic maps for a domain with loop is displayed in Figure 10.



Figure 10 The cyclographic map for a closed domain with loop (a) boundary curve with MAT (b) Cyclographic Map

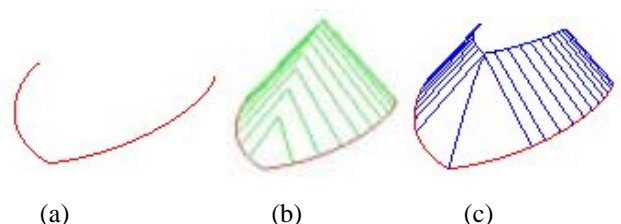
#### 4.4 From MAT Curves to its original closed boundary curve

As mention in the first section, the footpoint of the MAT point may be found from its MAT curve. We may find all of the boundary points via the MAT curve and generated the original closed boundary curve. We use a queue and a stack to store two parts of the boundary curves. Notice that for the end point on the MAT curve, we have to produce the (weighted) partial cone to connect two boundary points, after connect the boundary points, a list of points has to pop from the stack so that the boundary points are in order. The weighted partial cone is produced by linear interpolation by the angle of the cone, and angle between the line connect the MA point to its two boundary points.

#### 4.5 Blending at the vertex

The blending at the concave/convex vertex fix radius blending is produced by truncating the medial axis transform in the cyclographic map below  $z=r$  plane, and generated the region of the truncated medial axis transform (as Figure 11) The input boundary curve is generated by two Bezier curves whose control points are  $(-1.5,1.0,0.0), (-1.5,0.5,0.0), (-1.0,-1.5,0.0), (0.0,-2.0,0.0)$  and  $(0.0,-2.0,0.0), (1.0,-1.5,0.0), (1.5,0.5,0.0), (1.5,1.0,0.0)$  respectively. Notice that in this process, we generated a cone for the end points (cut by  $z=r$  plane), so that when we generate the region for the truncated medial axis transform, the corner is smooth. The blending at the concave vertex is similar. Notice that process is only work on vertices. It is not work for the case that  $z=r$  cut the medial axis transform in the cyclographic map at a branch without any end point.

The various radius blending is produced by truncating the weighted medial axis transform in the weighted cyclographic map below  $z=r$  plane, and generated the region of the truncated medial axis transform (as Figure 12). The control points for the boundary curve is the same as the on in Figure 11, except the weighted function for the first curve is  $\omega(t)=(1-t)*45^\circ+t*50^\circ$  and for the second curve is  $\omega(t)=(1-t)*55^\circ+t*60^\circ$ .



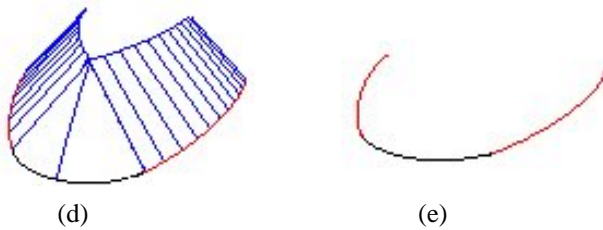


Figure 11 The blending at the convex vertex (a) Original curve (b) cyclographic map (c) cut by  $z=r$  (d) produce the cone (e) back to  $z=0$  plane



(a) Original curve (b) blending at the vertex

Figure 12 The various radius blending

## 5. REFERENCES

- 1] Bruce and Giblin, "Curve and Surface".
- 2] R. T. Farouki and C. A. Neff. Analytic properties of plane offset curves. *Computer Aided Geometric Design*, 7:83--100, 1990.
- 3] C. M. Hoffmann. *Geometric and Solid Modeling*. Morgan Kaufmann, San Mateo, Cal., 1989.
- 4] J. Hoschek. *Grundlagen der Geometrischen Datenverarbeitung*. Teubner Verlag, Stuttgart, 1989.
- 5] H. Blum. A transformation for extracting new descriptors of shape. In W. Whaten-Dunn, editor, *Models for the Perception of Speech and Visual Form*, pages 362--380. MIT Press, Cambridge, MA, 1967.
- 6] Christoph M. Hoffmann. Computer vision, descriptive geometry and classical mechanics. In B. Falcidieno and I. Hermann, editors, *Computer Graphics and Mathematics*. Springer Verlag, 1992.
- 7] Harry Blum, *Biological Shape and Visual Science (Part I)*, *Journal Theoretical Biology*, 38:205-287, 1973.
- 8] Azriel Rosenfeld and John L. Pfaltz, *Sequential Operations in digital Picture Processing*, *Journal of ACM*, 13(4):471-491, 1966.
- 9] John L. Pfaltz and Azriel Rosenfeld, *Computer Representation of Planar Regions by Their Skeleton*, *Communications of the ACM*, 10(2):119-125, 1967.
- 10] C. Judith Hilditch, *Linear Skeletons from Square Cupboards*, *Machine Intelligence*, 3:325-420, 1968.
- 11] Otis Philbrick, *Shape Description with the Medial Axis Transformation*, *Pictorial Pattern Recognition*, pages 395-407, Thompson Book Co. 1968.
- 12] Harry Blum and Roger N. Nagel, *Shape Description Using Weighted Symmetric Axis Features*, *Pattern Recognition*, 10:167-180, 1978.
- 13] Halit Nebi Gursoy, *Shape Interrogation by Medial Axis Transform for Automated Analysis*, Ph.D. Thesis.
- 14] N.M.. Patrikalakis and H.N. Gursoy, *Shape interrogation by Medial Axis Transform*, Technical Report, Design Lab. Memo. 90-2, Sea Grant College Program, MIT, 1990.
- 15] T.K.H Tam and C.G. Armstrong, *2D Finite Element Mesh Generation by Medial Axis Subdivision*, 1992.
- 16] V. Srinivasan, L. Nackman, J. Tang and S. Meshkat, *Automatic mesh generation using the symmetric axis transformation of polygonal domains*, Technical Report RC 16132, IBM Yorktown Heights, 1990.
- 17] Sabine Stifter, *The Roider method: A method for static and dynamic collision detection*, In C. Hoffmann, editor, *Issues in Robotics and Nonlinear Geometry*, JAI press, 1990.
- 18] C.N. Chu, R.L.Kashyap, T.C Lee and I.C. You, *Castability Evaluation via keleton-Based Modeling*, *CIDMAC Annual Report*, Schools of Engineering, Purdue University, 1990-1991.
- 19] Christoph M. Hoffmann and George Vanecek, Jr., *Fundamental Techniques for Geometric and Solid Modelling*, In C.T. Leondes, editors, *Advances in Control and Dynamics*. Academic Press, 1991.
- 20] E. Müller and J. Krames. *Die Zyklographie*. Franz Deuticke, Leipzig und Wien, 1929.
- 21] J. Plucker. On a new geometry of space. *Phil. Trans R. Soc.*, 155, 1865.
- 22] Christoph M. Hoffmann, A dimensionality paradigm for surface interrogations. *CAGD*, 7:517--532, 1990.
- 23] Rida T. Farouki and Jean-Claude A. Chastang. Evolving wavefronts as algebraic curves, Technical Report Technical Report RC-16381, IBM Yorktown Heights, 1990.
- 24] R. T. Farouki, The approximation of nondegenerate offset surfaces, *Computer Aided Geometric Design*, 3:15--43, 1986.
- 25] R. T. Farouki and C. A. Neff., Algebraic properties of plane offset curves. *Computer Aided Geometric Design*, 7:101--128, 1990.
- 26] J. Hoschek, Offset curves in the plane, *Computer Aided Design*, 17:77--82, 1985.
- 27] J. Hoschek and N. Wissel, Optimal approximate conversion of spline curves and spline approximation of offset curves. *Computer Aided Design*, 20:475--483, 1988.
- 28] Ching-Shoei Chiang, *The Euclidean Distance Transform*, Ph.D. Thesis, Department of Computer Science, August, 1992.
- 29] Hyeong In Choi, Sung Woo Choi, Hwan Pyo Moon and Nam Sook Wee, *New Algorithm for Medial Axis Transform of Plane Domain*, Technique Report RIM-GARC Preprint Series 95-88, Department of Mathematics, Seoul National University.
- 30] Hyeong In Choi, Sung Woo Choi and Hwan Pyo Moon, *Mathematical Theory of Medial Axis Transform*, Technique Report RIM-GARC Preprint Series 95-87, Department of Mathematics, Seoul National University.